FOCUS REVIEW

Electrochemical Materials and Technologies

eISSN: 2949-0561

Cite this: Electrochem. Mater. Technol. 3 (2024) 20243043

Progress in forming thin-film solid electrolytes based on $Li_7La_3Zr_2O_{12}$ by tape casting

Efim Lyalin [a]*, Evgeniya Il'ina [a]

Received: 30 July 2024
Accepted: 17 September 2024
Published online: 26 September 2024

DOI: 10.15826/elmattech.2024.3.043

All-solid-state batteries are in great demand worldwide. Particular attention is paid to the development of materials and the design of these batteries. Solid electrolytes have lower total conductivity compared to liquid electrolytes, so it is assumed that the transition to thin-film electrolytes can significantly reduce the internal resistance of the cell. Solid electrolytes of the garnet family based on $Li_7La_3Zr_2O_{12}$ (LLZ) are considered as promising ceramic membranes for such power sources. In the presented review, different methods for film formation of LLZ and their features are discussed. The tape casting method is considered in more detail as a promising approach for the formation of thin films of LLZ. The slurry components and heat treatment conditions for the formation of solid electrolyte films with thicknesses ranging from 10 to 500 μm and high values of conductivity (10^{-3}–10^{-4} S · cm^{-1} at room temperature) are analyzed. Thus, the tape casting method can be used to obtain films with lithium-ion conductivity and relative density values comparable to those of bulk ceramic samples. However, the problem of organizing the electrode | solid electrolyte interface and the design of all-solid-state batteries remains very relevant for their development.

keywords: $Li_7La_3Zr_2O_{12}$, lithium-ion conductivity, tape casting, thin films, all-solid-state battery

1. Introduction

Energy consumption is constantly growing, as energy is crucial in many areas of human life. Electricity production is a continuous process, but human consumption usually changes cyclically every day. Therefore, the generated energy should be accumulated for further use. Electrochemical energy storage devices and energy converters (batteries) are the most convenient devices for storing and generating energy. Lithium-ion batteries possess the highest values of energy density among them.

Such power sources contain liquid (or gel-like) electrolytes, that are based on a solution of lithium salt in an aprotic solvent. However, liquid electrolytes may become thermally unstable if operating parameters are exceeded. In this case, irreversible reactions of the electrolyte with the electrode materials may occur, which can lead to gas formation and explosion of the battery. The transition from liquid to solid electrolytes is considered to be one of the solutions to this problem [1–5].

A promising family of lithium-ion conductors with a garnet structure can be considered as a lithium-ion solid electrolyte for all-solid-state batteries (ASSB) [6–8]. In 2007, R. Murugan et al. synthesized a new compound with a garnet structure, $Li_7La_3Zr_2O_{12}$ (LLZ) [9]. This solid electrolyte with a cubic structure has not only the highest lithium-ion conductivity of $3.0 \cdot 10^{-4}$ S · cm^{-1} at 25 °C, but also chemical stability versus lithium metal.

The $Li_7La_3Zr_2O_{12}$ compound has two modifications: tetragonal (10^{-6}–10^{-7} S · cm^{-1} at room temperature (RT)) and cubic (10^{-3}–10^{-4} S · cm^{-1} at RT) [10, 11]. In recent years, thanks to the doping of this compound in various sublattices, and optimization of the synthesis technique, it has been possible to obtain highly conductive compositions reaching lithium-ion conductivity values of around 10^{-3} S · cm^{-1} at RT [10–12].

One of the difficulties in the transition to solid electrolytes is their low total conductivity compared to

a: Institute of High-Temperature Electrochemistry of Ural Branch of RAS, Ekaterinburg 620137, Russia

* Corresponding author: lyalin@ihte.ru

liquid ones, which forces them to be converted into thin-film materials [13–15]. Thin films are widely used as various functional coatings: to increase strength, corrosion resistance, as well as to improve the magnetic and electrical properties of materials in aviation, medicine, electrical engineering, and other areas. The use of thin-film materials makes it possible to miniaturize and reduce the material consumption of various devices.

In the case of power sources, thin film electrolytes can significantly reduce the internal resistance of the cell. However, in the industry, there is currently no established technology for producing lithium-conducting materials of the required composition in the form of thin films. Thus, the development of thin-film technologies is important for the advancement of devices for generating and storing electricity, and it is one of the priority areas in improving energy efficiency, particularly in power plants based on solid oxide fuel cells and chemical power sources.

1.1. Methods for producing solid electrolytes based on $Li_7La_3Zr_2O_{12}$ in the form of thin films

According to the literature, there are many different methods for producing solid electrolytes based on LLZ in the form of thin films. Conventionally, they can be divided into two groups: production from the gas phase and production from solution, as shown in Table 1. Moreover, the methods presented in Table 1 can also be divided according to other criteria. For example, some methods rely on the use of precursors, while other methods use a pre-synthesized compound. Alternatively, the methods can be divided according to the phase composition of the obtained coating: precursor films with an amorphous phase and films that have retained the modification of the original material.

The group of methods related to vapor deposition (VD) includes chemical and physical methods that involve the thin-film deposition from the gas phase of precursors or atoms of the compound, respectively (Table 1). The mechanism of this type of deposition promotes a uniform distribution of particles at the molecular level, which enables the production of ultrathin films.

For example, chemical methods are characterized by the deposition of films during a chemical reaction on the surface of the substrate. The chemical vapor deposition (CVD) method is based on the evaporation of volatile starting components, which are fed into a closed system with a carrier gas along with a reaction gas under certain conditions, Figure 1a. The reaction occurs under pressure on the surface of a heated substrate. In the literature, there are a number of works devoted to the formation of thin films of the solid electrolyte LLZ by this method [16–19]. For instance, H. Katsui et al. [16] obtained the LLZ film with a cubic structure by the CVD method. The mixture of evaporated precursors was fed into the reactor using Ar gas, and oxygen gas was supplied separately and mixed with the initial vapor above the substrate. The deposition temperature was 950 °C, and the total reactor pressure was maintained at 400 Pa. The obtained LLZ film with a thickness of ~ 5 μm possesses a lithium-ion conductivity of $1.4 \cdot 10^{-5}$ S · cm^{-1} at room temperature.

In turn, atomic layer deposition (ALD) is similar to the CVD process. However, in CVD all reactants are introduced simultaneously to create a film, while ALD is based on self-limiting vapor-phase half-reactions following one another (Figure 1a). Precursors are fed into the reactor one at a time, separated by periods of purging or evacuation. At each stage of exposure to a precursor, the surface is saturated with a monomolecular layer of this precursor. For example, in the work [20] Al-doped LLZ film was prepared by the ALD method. The oxide layers of each element were sequentially deposited on a Si(100) substrate by feeding a precursor and an oxidizing agent (O_3 - ozone) into the reactor. The obtained film with a thickness of 86.5 nm has an amorphous structure. Heating at 555 °C in a He atmosphere leads to the formation of a cubic structure, but upon cooling, the transition from cubic to tetragonal modification was observed. Thus, the obtained film was close to the specified stoichiometry $Li_{6.28}La_3Zr_2O_{12}Al_{0.24}$ and possesses low values of conductivity, $1 \cdot 10^{-8}$ S · cm^{-1} at 25 °C.

CVD and ALD methods allow obtaining thin films with thicknesses ranging from tens of nm to several μm and uniformly covering the developed surface. However, the disadvantages of these methods include expensive equipment, a low deposition rate, large losses of material, low productivity, and difficulties in selecting volatile precursors.

Physical methods are deposition processes in which the material is evaporated from a solid or liquid source as atoms or molecules and transported as vapor through a vacuum or low-pressure gaseous environment (or plasma) to a substrate where it condenses (Table 1).

Magnetron sputtering (MS) is a method of depositing particles that evaporate from a «target» using a non-thermal evaporation process. During this process, surface atoms are physically ejected from a solid surface through momentum transfer from an atomic-sized bombarding particle, which is typically a gaseous ion, accelerated by the plasma (Figure 1b). The plasma used in sputtering may be concentrated near the sputtering surface or may fill the space between the target and the substrate [21–23]. In the work of S. Lobe et al. [21], a method for producing an LLZ film using radio frequency magnetron sputtering in pure Ar plasma was presented. An Aluchrom YHf foil was used

Table 1 – Methods of thin-film formation.

	Vapor deposition (CVD)		Solution Deposition (SD)	
Method	•Chemical vapor deposition; •Atomic layer deposition	•Magnetron sputtering; •Pulsed laser deposition; •Suspension Plasma Spray	•Chemical solution deposition (dip-coating, spin-coating)	•Tape casting; •Electrophoretic deposition
Features	Initial components - volatile compounds	A particle source - compound (target)	Using a precursor solution	Suspension of solid particles from compound

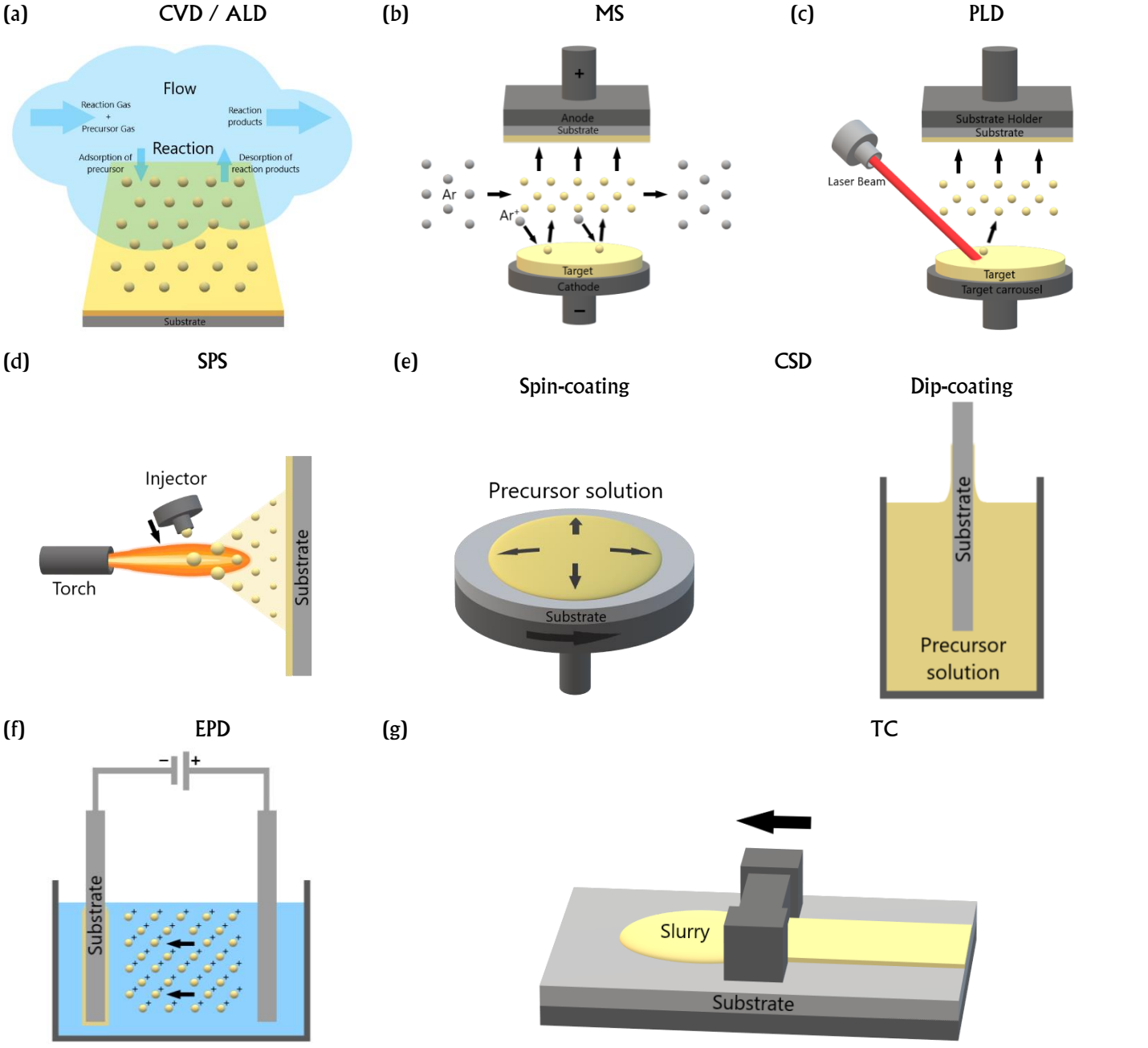

Figure 1 Schemes of different methods of thin-film formation.

as a substrate, and deposition was carried out at substrate temperatures ranging from 150 to 800 °C. At 700 °C, a cubic structure without impurities was obtained with a conductivity of $2 \cdot 10^{-9}$ and $1.2 \cdot 10^{-4}$ S · cm^{-1} at 25 °C in the cross-section and in the plane, respectively. The advantages of MS include the ability to produce ultra-thin films with thicknesses of several nm, a small number of defects, and the accurately reproduced chemical composition. The disadvantages of MS include the high cost of equipment and the amorphous phase of the obtained film.

Pulsed laser deposition (PLD) is a process in which material from a thermal evaporation source reaches a substrate virtually without collision with gas molecules in the space between the source and the substrate (Figure 1c). It should be noted that the rate of thermal evaporation can be very high compared to other evaporation methods. The material evaporating from the source has a composition that is proportional to the relative vapor pressure of the material in the molten state. Thermal evaporation is carried out using a high-energy electron beam (e-beam), which heats the source material. Typically, the substrates are installed at a considerable distance from the evaporation source to reduce heating of the substrate by the evaporation source [24, 25]. In the work of M. Rawlence et al. [24], LLZ films were deposited by the PLD method. The films were deposited on an MgO substrate at a distance of 65 mm from the target. After deposition the LLZ film with a thickness of 380 nm has an amorphous structure. The obtained films were annealed at 600 °C for 24 h in the presence of LiOH. The LLZ film has a cubic structure and low values of conductivity, $1.2 \cdot 10^{-3}$ S · cm^{-1} at 325 °C. PLD has high productivity, a high deposition rate, and the ability to reproduce the chemical composition. However, there are some difficulties in thickness control and producing uniform thin films over a large area.

The Suspension Plasma Spray (SPS) process involves feeding a dispersed material into a high-temperature plasma jet (Figure 1d). The suspension then breaks down into small droplets, which dry to fine solid particles. They are sintered and melted in the process. Molten or semi-molten particles fly out of the burner nozzle, hit the substrate, and solidify on it. In the work of I. Koresh et al. [26], a suspension based on the cubic LLZ with 2.5 vol. % ethanol was sprayed with plasma onto stainless steel substrates. The highest conductivity value of $7.3 \cdot 10^{-6}$ S · cm^{-1} at 22 °C was shown by a film (15 μm) with a high content of the amorphous phase. It was assumed that the obtained amorphous phase plays a predominant role in the lithium-ion conductivity of the film. SPS also has a high deposition rate, but need the high cost of equipment. The obtained films have an amorphous phase.

A group of methods related to solution deposition (SD) involves the formation of a film from a solution. The mechanism for obtaining the coating is very different from that of VD and does not require the use of expensive equipment. The initial components may be in the form of a precursor solution or dispersed particles of the compound.

Chemical solution deposition (CSD) is a technique based on the preparation of a precursor solution with a selected concentration. This is achieved by mixing soluble starting components in a solvent. There are various methods of applying the precursor solution to a substrate, depending on the application conditions, such as dip-coating and spin-coating [27, 28]. For example, K. Tadanaga et al. [27] fabricated $Li_{7.7}La_3Zr_2Al_{0.3}O_{12}$ films on an MgO substrate using the dip-coating method. The precursor solution was prepared by mixing the soluble starting components in a given ratio. 0.1 wt. % lithium dodecyl sulfate (an ionic surfactant) was added to improve the surface morphology of the thin films. The as-deposited films were amorphous with a thickness of 1 μm and were then annealed at 450 °C for 15 min. After further annealing the film with Li_2CO_3 in an alumina crucible at 900 °C, the cubic structure of LLZ was obtained, with a small amount of $LaAlO_4$ impurity. The conductivity of the obtained thin film electrolyte was $2.4 \cdot 10^{-6}$ S · cm^{-1} at 25 °C. The advantages of CSD include easy control of the coating layer thickness and uniform deposition of thin films. However, the disadvantages are the amorphous phase of the as-deposited films, the labor-intensive nature, and the need to select soluble precursors.

Electrophoretic deposition (EPD) is based on the phenomenon of electrophoresis in a suspension of particles. In a dispersion medium, solid particles form micelles. The particle itself is electrically neutral, but potential-forming ions are adsorbed onto its surface. They attract proionics, forming an electrical double layer near the surface and a diffusion layer outside. Under an external electric field, particles with a double electric layer move towards the substrate electrode and form a thin coating. The ions of the diffusion layer move toward the counter electrode. For example, in our previous works [29, 30], $Li_7La_3Zr_2O_{12}$ films were first obtained by EPD on various metal substrates. The addition of crystalline iodine (0.4 g · L^{-1}) to a suspension of $Li_7La_3Zr_2O_{12}$ powder (10 g · L^{-1}) in an isopropanol/acetylacetone medium (70/30 vol. %) led to the formation of uniform films. The EPD process was carried out at a constant voltage (80 V) for 4 minutes between the electrodes (distance 10 mm). The $Li_7La_3Zr_2O_{12}$ film (~ 30 μm thick) had a tetragonal

structure after drying and a cubic structure after heat treatment at 300 °C in an Ar atmosphere. The lithium-ion conductivity of the LLZ films annealed at 300 °C was equal to $1.1 \cdot 10^{-8}$ S · cm^{-1} at 100 °C. Thus, a solid electrolyte film with a thickness of several μm can be obtained by EPD, but only on a conductive substrate. Moreover, the obtained LLZ films had low conductivity values.

It can be concluded that considered methods for the formation of thin films of solid electrolytes based on LLZ have some disadvantages: the complexity of obtaining precursors, the long duration of the process, the amorphous phase of the obtained film, dramatic loss of lithium during the deposition process or heat treatment, and the requirement for high-precision and expensive equipment. This has led to the complication and increase in the cost of the technological process for obtaining thin films of solid electrolyte.

Tape casting is based on the mechanical formation of a film by smoothing the slip mass using a doctor blade with a certain gap. The binder and the plasticizer form a polymer matrix with the particles of the solid electrolyte after the solvent evaporation. The obtained film is flexible and mechanically strong. The tape casting method can be considered as a promising technique for the formation of thin films of LLZ. It is widely known that tape casting is an inexpensive method for producing thin ceramic sheets of large area and thickness in the range of 0.025 to 1.27 mm [31]. Moreover, it should be noted that this method is easy to adapt for industrial production. For example, the tape casting process is often used in industry for the production of corundum substrates and various ceramic materials. The preparation scheme and the obtained $Li_7La_3Zr_2O_{12}$ film are shown in Figures 2a and b, respectively.

In order to obtain a uniform film from a ceramic powder used in tape casting, it is necessary to add a solvent, binder, plasticizer, and dispersant. The solvent promotes the uniform distribution of all components within its volume, and there are certain requirements for the solvent. The solvent must be able to distribute the powder particles evenly, evaporate quickly, and be non-toxic.

The powder added to the solution is usually in the form of agglomerates or flakes, which can trap air in the interstitial space between the particles. Trapped air can cause problems with air removal during the later stages of slurry preparation. As a result, the introduced binder envelops a group of particles rather than individual particles.

Therefore, the use of a dispersant prevents the particles from sticking together, thereby increasing the uniformity of the slurry and the freshly cast tape.

The binder is one of the important components of the slurry due to its ability to form a network that holds the entire system together, acting as a matrix and enveloping the ceramic material. The binder, being the continuous phase, has the greatest influence on the properties of the freshly cast tape such as strength, flexibility, ductility, and moldability. When choosing a binder for tape casting, attention should be paid to factors such as solubility, viscosity, strength, burnout temperature, bottom ash, and firing atmosphere.

Since the tape after casting is subjected to mechanical processing, the purpose of the plasticizer is to impart flexibility to the tape (reduce stress), thereby suppressing the formation of cracks in the material. The plasticizer should combine well with the other organic components in the system, form stable compositions with them, and have low volatility. Without the addition of plasticizers, the binder system would form a rigid, brittle film structure that is prone to cracking and failure during the mechanical processing steps. The plasticizers help to maintain the necessary flexibility and integrity of the tape, allowing it to withstand the stresses encountered during cutting, bending, and other shaping operations.

Moreover, it should be noted that all the above-mentioned components of the slurry should be mixed in a certain order and ratio [31]. The quality of the film directly depends on the ratio of the additives. A green tape without the addition of the required amount of plasticizer will be highly susceptible to deformation since it dries unevenly. The solvent evaporates intensively from the outside of the film, while it leaves slowly from the substrate side. So, internal stresses can be created, which can lead to various defects such as curling, cracking, etc. (Figure 2c). On the other hand, an excessive amount of plasticizer greatly reduces the yield strength of the slip and increases the adhesion of the film to the substrate surface. This leads to problems with film removal from the substrate. Moreover, particular attention should be paid to the viscosity of the slurry. For example, it is difficult to remove gas from a thick slurry, which leads to the formation of pores on the film surface (Figure 2d).

According to the literature data, before casting the obtained slurry onto the substrate, in some cases, a process of degassing by mixing the slurry in a vacuum chamber is described [37–43, 47]. In other works, the degassing process is not described; it can be assumed that the selection of the slurry components and the conditions for its preparation allow casting the slurry without degassing and obtaining defect-free LLZ films. The stirring of the slurry without grinding media was carried out to remove residual air and prevent the thixotropy effect before it was cast onto the substrate.

In Table 2, the slurry components that are most often used to prepare LLZ films by tape casting are listed. According to the literature data, Polyvinyl butyral and Benzyl butyl phthalate are used more often as the binder and plasticizer, respectively. Uniform LLZ films with a thickness ranging from 10 to 500 μm were obtained using these components.

Table 2 – Slurry components for tape casting films of solid electrolytes based on LLZ.

Solid electrolyte	Binder	Plasticizer	Dispersant	Solvent	Reference
$Li_{6.25}Al_{0.25}La_3Zr_2O_{12}$ (37 wt. %)	Polyvinyl butyral (3 wt. %)	Benzyl butyl phthalate (3 wt. %)	Polyacrylic acid (2 wt. %)	Ethanol + acetone (29 + 29 wt. %)	[32]
$Li_{6.25}Ga_{0.25}La_3Zr_2O_{12}$ (37 wt. %)	Polyvinyl butyral (3 wt. %)	Benzyl butyl phthalate (3 wt. %)	Polyacrylic acid (1 wt. %)	Ethanol + acetone (28 + 28 wt. %)	[33]
$Li_{6.9}La_3Zr_{1.95}Zn_{0.05}O_{12}$	Polyvinyl butyral (8 wt. %)	Benzyl butyl phthalate + + polyethylene glycol (5 + 2.5 wt. %)	Fish oil (3 wt. %)	Ethanol + xylene + + toluene	[34]
$Li_7La_{2.75}Ca_{0.25}Zr_{1.75}Nb_{0.25}O_{12}$	Polyvinyl butyral	Benzyl butyl phthalate	Fish oil	Isopropanol + toluene	[35, 36]
$Li_7La_3Zr_{1.75}Nb_{0.25}Al_{0.1}O_{12}$ (40–45 wt. %)	Ethyl cellulose (2–3 wt. %)	Polyethylene glycol 400 + + dibutyl phthalate (0.5–1 + + 1–2 wt. %)	Fish oil (1–2 wt. %)	Ethanol + toluene (45–55 wt. %)	[37]
$Li_{6.4}La_3Zr_{1.4}Ta_{0.6}O_{12}$ (50 wt. %)	Acrylic resin (6 wt. %)	Methyl benzoate (2 wt. %)	–	Ethanol + butyl acetate (12 + 12 wt. %)	[38]
$Li_{6.75}La_{2.75}Ca_{0.25}Zr_{1.5}Nb_{0.5}O_{12}$ (23 wt. %)	Polyvinyl butyral (4 wt. %)	Benzyl butyl phthalate (5 wt. %)	Fish oil (0.5 wt. %)	Isopropanol + toluene (16 + 16 wt. %)	[39]
$Li_{6.45}Al_{0.05}La_3Zr_{1.6}Ta_{0.4}O_{12}$ (52.40 wt. %)	Methyl cellulose (0.44 wt. %)	Polyethylene glycol + glycerol (1.75 + 1.75 wt. %)	–	Deionized H_2O (43.66 wt. %)	[40]
$Li_7La_{2.75}Ca_{0.25}Zr_{1.75}Nb_{0.25}O_{12}$ (23 wt. %)	Polyvinyl butyral (4 wt. %)	Benzyl butyl phthalate (5 wt. %)	Fish oil (0.5 wt. %)	Isopropanol (32 wt. %)	[41]
$Li_6Ga_{0.15}Al_{0.1}La_3Zr_{1.75}Ta_{0.25}O_{12}$	Polyvinyl butyral	Diamine	Adipic acid	Toluene + 1-butanol	[42]
Commercial Al-doped LLZ (37 wt. %)	Polyvinyl butyral (5 wt. %)	Benzyl butyl phthalate (5 wt. %)	Fish oil (0.5 wt. %)	Isopropanol + toluene (15 + 15 wt. %)	[43]
$Li_{6.5}La_3Zr_{1.5}Ta_{0.5}O_{12}$ (34.48 wt. %)	Polyvinyl butyral (5.81 wt. %)	Benzyl butyl phthalate (5.08 wt. %)	Fish oil (0.91 wt. %)	Isopropanol + toluene (26.86 + 26.86 wt. %)	[44]
$Li_7La_{2.75}Ca_{0.25}Zr_{1.75}Nb_{0.25}O_{12}$	Polyvinyl butyral	Benzyl butyl phthalate	Fish oil	Isopropanol	[45]
$Li_{6.4}La_3Zr_{1.4}Ta_{0.6}O_{12}$ (40 wt. %)	Polyvinyl butyral (5 wt. %)	Benzyl butyl phthalate (5.5 wt. %)	Fish oil (3 wt.%)	Ethanol + xylene (31 + 15.5 wt. %)	[46]
$Li_{6.25}Al_{0.25}La_3Zr_2O_{12}$ + + 3 wt. % MgO (45.6 wt. %)	MSBI-13 (13.3 wt. %)	–	DS002 (1 wt. %)	Toluene (40.1 wt. %)	[47]

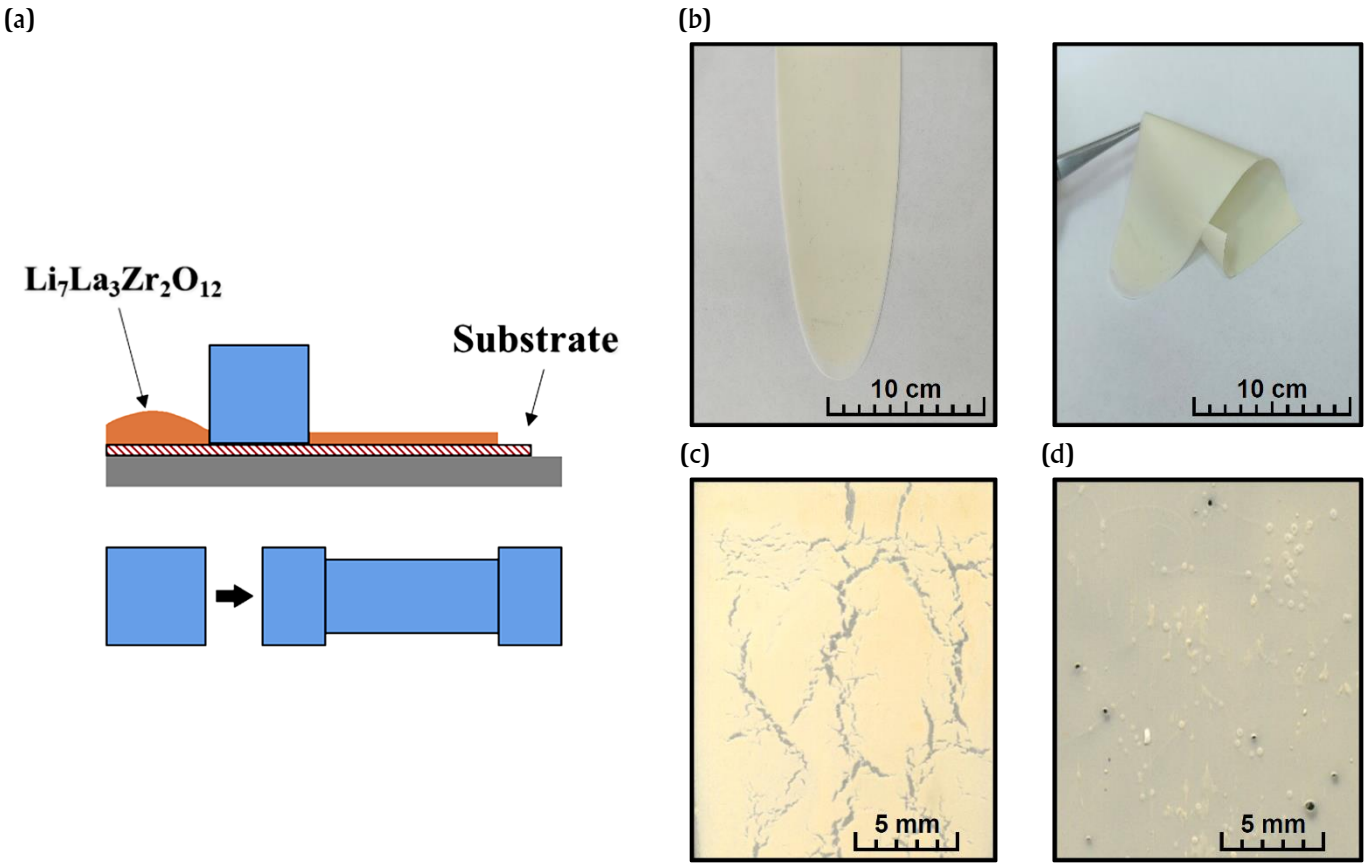

Figure 2 (a) The scheme of tape casting the on the mylar; (b) dried LLZ film; (c, d) defects in LLZ films.

1.2. Target characteristics of LLZ thin films produced by tape casting

The heat treatment conditions, film thickness, density, and conductivity of the film solid electrolytes based on LLZ formed by tape casting are presented in Table 3. In some works [34, 39, 42–44], single-layer films were investigated as solid electrolytes. The slurry was usually cast onto the substrate, and after drying, the film was removed and annealed under various conditions. For example, in work [34], a $Li_{6.9}La_3Zr_{1.95}Zn_{0.05}O_{12}$ film was cast on a polyvinyl chloride (PVC) substrate. The cast film was dried at room temperature, removed from the substrate, and then cut into disks with a diameter of 10 mm. The prepared samples after the final sintering stage (1250 °C, 5 h) had a thickness of ~ 500 μm, a density of ~ 85 %, and a total conductivity of $8 \cdot 10^{-5}$ S · cm^{-1} at room temperature. In [42], a $Li_6Ga_{0.15}Al_{0.1}La_3Zr_{1.75}Ta_{0.25}O_{12}$ film was cast onto a polyester film (substrate). The dried film was removed from the substrate and sintered at 1100 °C for 4 h in air. The relative density of the obtained solid electrolyte reached 91 %. After annealing, the film thickness was 110 μm, and the conductivity was $6.7 \cdot 10^{-4}$ S · cm^{-1} at room temperature. To increase the density and conductivity of LLZ, hot pressing was used in [32, 33, 35, 36, 38, 45]. For example, in work [33], the cast film was removed from the Mylar substrate and hot pressed at a temperature of 80–100 °C and a pressure of 50–70 MPa for 5–10 min. The pressed samples were then sintered at a final temperature of 1130 °C in N_2 between graphite substrates. After annealing, the thickness of the solid electrolyte film was ~ 25 μm, with a density of 95 % and a conductivity of $1.3 \cdot 10^{-3}$ S · cm^{-1}.

The hot pressing was also used to obtain multilayer films with a thickness (> 50 μm) by combining several layers of solid electrolyte [37, 40, 41, 46, 47]. For example, in work [37], the dried film had a thickness of ~ 60 μm. Hot-pressed 6-layer samples had a thickness of ~ 200–250 μm and a density of 60–62 %. After the final sintering stage (1000 °C), the thickness of the films was 150–170 μm. The density and total conductivity of the obtained samples reached ~ 90 % and $1.5 \cdot 10^{-4}$ S · cm^{-1}, respectively.

Thus, it can be seen that solid electrolyte films with a thickness ranging from 10 to 200 μm possess high values of conductivity (10^{-3}–10^{-4} S · cm^{-1} at room temperature) and relative density (> 90 %) typical for bulk ceramic samples. Sufficiently high final heat treatment temperatures (> 1000 °C) are required to obtain such high target material characteristics. There was a problem

Table 3 – Heat treatment conditions, thickness, total conductivity and density of thin-film solid electrolytes based on LLZ obtained by tape casting.

Solid electrolyte	Heat treatment conditions	Thickness, μm	Total conductivity at RT, $S \cdot cm^{-1}$	Density, %	Reference
$Li_{6.25}Al_{0.25}La_3Zr_2O_{12}$	1090 °C, 1 h, N_2, between graphite foil; 800 °C, 1–4 h, O_2, on MgO plates	< 30 (1 layer)	$2 \cdot 10^{-4}$	94	[32]
$Li_{6.25}Ga_{0.25}La_3Zr_2O_{12}$	1130 °C, 0.3 h, N_2, between graphite foil; 900 °C, 2 h, N_2, between graphite foil; 800 °C, 1–4 h, O_2, on MgO plates	25 (1 layer)	$1.3 \cdot 10^{-3}$	95	[33]
$Li_{6.9}La_3Zr_{1.95}Zn_{0.05}O_{12}$	600 °C, 1 h, air; 1250 °C, 5 h, air	500 (1 layer)	$8 \cdot 10^{-5}$	80-90	[34]
$Li_7La_{2.75}Ca_{0.25}Zr_{1.75}Nb_{0.25}O_{12}$	700 °C, 4 h; 1100 °C	35 (1 layer)	$2.2 \cdot 10^{-4}$	–	[35]
$Li_7La_{2.75}Ca_{0.25}Zr_{1.75}Nb_{0.25}O_{12}$	1100 °C, 6 h	20 (1 layer)	$2.2 \cdot 10^{-4}$	–	[36]
$Li_7La_3Zr_{1.75}Nb_{0.25}Al_{0.1}O_{12}$ + + 0.5 wt. % Li_3BO_3	650 °C, 1 h, air; 1000 °C, 6 h, Ar	150 (6 layers)	$2.83 \cdot 10^{-4}$	90	[37]
$Li_{6.4}La_3Zr_{1.4}Ta_{0.6}O_{12}$	650 °C, 1 h, air; 1100 °C, 6 h, air, covered with mother powders.	200 (1 layers)	$5.2 \cdot 10^{-4}$	99	[38]
$Li_{6.75}La_{2.75}Ca_{0.25}Zr_{1.5}Nb_{0.5}O_{12}$	1050 °C, 1 h	~ 10 (1 layer)	–	–	[39]
$Li_{6.45}Al_{0.05}La_3Zr_{1.6}Ta_{0.4}O_{12}$	700 °C, 1 h, air, between MgO plates in a closed alumina crucible; 1175 °C, 4 h, air, between MgO plates in a closed alumina crucible; 800 °C, 1 h, Ar, on an alumina boat	150 (2 layers)	$1.5 \cdot 10^{-4}$	90	[40]
$Li_7La_{2.75}Ca_{0.25}Zr_{1.75}Nb_{0.25}O_{12}$	700 °C, 4 h; 1050 °C, 1 h.	50 (3 layers)	$2.12 \cdot 10^{-4}$	> 99	[41]
$Li_6Ga_{0.15}Al_{0.1}La_3Zr_{1.75}Ta_{0.25}O_{12}$	1100 °C, 4 h, air	110 (1 layer)	$6.7 \cdot 10^{-4}$	91	[42]
Commercial LALZO	600 °C, 12 h, Ar; 1100 °C, 12 h, Ar.	20 (1 layer)	–	> 90	[43]
$Li_{6.5}La_3Zr_{1.5}Ta_{0.5}O_{12}$	1100 °C, 10 min, air, in MgO crucible	12–15 (1 layer)	$1.19 \cdot 10^{-3}$	–	[44]
$Li_7La_{2.75}Ca_{0.25}Zr_{1.75}Nb_{0.25}O_{12}$	700 °C, 4 h, 1050 °C, 1 h,	50 (1 layer)	$2.12 \cdot 10^{-4}$	99	[45]
$Li_{6.4}La_3Zr_{1.4}Ta_{0.6}O_{12}$	300 °C 500 °C 1050 °C, 2 h, air 1260 °C, 12 h, air	83 (multi-layer)	$2.0 \cdot 10^{-5}$	–	[46]
$Li_{6.25}Al_{0.25}La_3Zr_2O_{12}$ + + 3 wt. % MgO	1115 °C for 3 h	100 (4 layers)	$4.35 \cdot 10^{-4}$	87.8	[47]

of high loss of lithium oxide during heat treatment, which leads to a low conductivity of LLZ films [45]. However, this problem was successfully solved by hot pressing of several layers of cast tape followed by sintering under a mother of lithium-containing phase, or between different substrates.

In the Table 3, there are some studies on the creation of composite thin-film solid electrolytes [37, 47]. For example, R.A. Johnson et al. [37] investigated the effect of the Li_3BO_3 additive on the conductivity of the $Li_7La_3Zr_{1.75}Nb_{0.25}Al_{0.1}O_{12}$ thin-film electrolyte. The composite solid electrolyte with a 0.5 wt. % Li_3BO_3 addition, annealed at 1000 °C for 6 h, had maximum values of total conductivity ($2.83 \cdot 10^{-4}$ S · cm^{-1}). The introduction of a larger Li_3BO_3 amount led to a decrease in conductivity due to an increase in grain boundary resistance, which indicates an increased presence of Li_3BO_3 at grain boundaries. The thin-film solid electrolyte without the additive had slightly lower total conductivity ($1.28 \cdot 10^{-4}$ S · cm^{-1}), but higher density values (92.3 %) and significantly greater grain boundary strength than the composites. However, it was shown that thin-film composite electrolytes based on LLZ with Li_3BO_3 addition can be sintered without the use of sacrificial powder covering. Thus, the addition of Li_3BO_3 can also prevent the high loss of lithium oxide from LLZ films during annealing. In work [47], MgO was investigated as a sintering additive to improve ionic conductivity and density of the thin-film solid electrolyte based on LLZ. However, it was established that the introduction of MgO additive to $Li_{6.25}Al_{0.25}La_3Zr_2O_{12}$ does not lead to a significant increase in the density and total conductivity of thin-films obtained by tape casting. It should be noted that B. Dai et al. [46] also used MgO as a sintering aid during slurry preparation, but its quantity and influence on the properties of the LLZ film were not discussed.

A prototype of ASSB based on the thin-film electrolyte $Li_7La_{2.75}Ca_{0.25}Zr_{1.75}Nb_{0.25}O_{12}$, obtained by tape casting, with $Li(Ni_{0.5}Mn_{0.3}Co_{0.2})O_2$ (NMC) cathode and Li anode was assembled and tested [36]. A feature of the technological assembly was the production of dense and porous layers by tape casting, which were then laminated into a bilayer tape. Poly(methyl methacrylate) spheres were added to the slurry to fabricate the porous sheets. The interface between the porous side of the solid electrolyte and the Li anode was modified by a zinc oxide coating. After heating at 250 °C, the Li formed an alloy with the zinc oxide and infused into the porous framework (Figure 3). The interface between the dense side of the solid electrolyte and the NMC cathode was modified by a gel electrolyte. Moreover, a liquid electrolyte (1 M $LiPF_6$ in ethylene carbonate: diethyl carbonate) was injected into

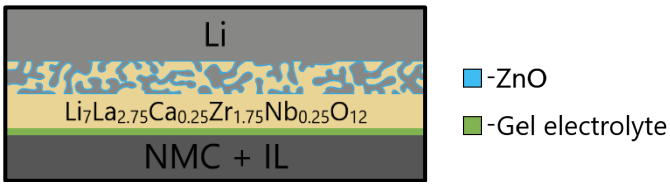

Figure 3 Scheme of the assembled NMC | thin-film electrolyte $Li_7La_{2.75}Ca_{0.25}Zr_{1.75}Nb_{0.25}O_{12}$ | Li cell.

the cathode. Such modifications led to stable cycling of the assembled cells with discharge capacities of ~ 175 mAh/g at a 0.1 C rate. Thus, the prospects and possibilities of using the tape casting method for the formation of high-density and highly conductive thin-film electrolytes based on LLZ, as well as porous structures, have been demonstrated.

2. Conclusions

Currently, a large number of methods have been proposed for the formation of solid electrolyte membranes based on LLZ in the form of thin films. According to the literature data, each method has its own advantages and disadvantages. In the presented review, the promise of using the Tape Casting method is shown in terms of its low cost and ease of applicability for future production processes.

To obtain a uniform film from a ceramic powder used by the tape casting method, it is necessary to add a solvent, binder, plasticizer, and dispersant. According to the literature data, Polyvinyl butyral, Butylbenzyl phthalate, fish oil, and mixtures based on ethanol or isopropanol are more commonly used as the binder, plasticizer, dispersant, and solvent, respectively. It is necessary to select the correct ratio of components for the used ceramic powder to ensure the required viscosity, as failure to comply with these conditions can lead to the formation of various film defects.

According to the literature data, thin films with thicknesses ranging from 10 to 500 μm can be obtained for LLZ family solid electrolytes by tape casting. Most often, films with a thickness from 10 to 50 μm are cast, and several layers of these can be hot-pressed to increase the density and conductivity of the thin-film electrolyte.

To prevent a high loss of lithium oxide from the LLZ film during heat treatment, sintering additives should be introduced, or annealing should be carried out under a mother of lithium-containing phase, or between different substrates. The use of the tape casting method with subsequent heat treatment makes it possible to obtain thin ceramic membranes with high relative densities > 90 % and conductivity around 10^{-3}–10^{-4} S · cm^{-1} at room temperature. It can be concluded that LLZ-based films

with conductivity values close to those of bulk samples can be obtained by the tape casting method.

It was shown that the tape casting technique provides prospects and opportunities for creating both dense and porous films, which can be used for technological solutions in the formation of electrochemical devices. However, the problem of organizing the interface between the electrodes and the solid electrolyte still remains very relevant for ASSB development.

Supplementary materials

No supplementary materials are available.

Funding

This work was supported by the Research Program N◦ 122020100210–9 (IHTE UB RAS), Russian Academy of Sciences, Ural Branch, Russia.

Author contributions

Efim Lyalin: Conceptualization; Data curation; Writing – Original draft; Writing – Review & Editing; Formal Analysis; Software; Visualization.

Evgeniya Il'ina: Conceptualization; Writing – Original draft; Writing – Review & Editing.

Conflict of interest

The authors declare no conflict of interest.

Additional information

Author IDs:
Lyalin E.D.
Scopus ID 57213417781;
ORCID 0000-0002-0539-506X.
Il'ina E.A.
Scopus ID 54782709600;
ORCID 0000-0003-1759-5234.

References

1. Wu X, Ji G, Wang J, Zhou G, et al., Toward Sustainable All Solid-State Li–Metal Batteries: Perspectives on Battery Technology and Recycling Processes, Adv. Mater., **35(51)** (2023) 2301540. https://doi.org/10.1002/adma.202301540

2. Zhang C, Hu Q, Shen Y, Liu W, Fast-Charging Solid-State Lithium Metal Batteries: A Review, Adv. Energy Sustain. Res., **3(6)** (2022) 2100203. https://doi.org/10.1002/aesr.202100203

3. Xia S, Wu X, Zhang Z, Cui Y, et al., Practical challenges and future perspectives of all-solid-state lithium-metal batteries, Chem., **5(4)** (2019) 753–785. https://doi.org/10.1016/j.chempr.2018.11.013

4. Wu D, Chen L, Li H, Wu F, Solid-state lithium batteries-from fundamental research to industrial progress, Prog. Mater. Sci., **139** (2023) 101182. https://doi.org/10.1016/j.pmatsci.2023.101182

5. Wang C, Sun X, The promise of solid-state batteries for safe and reliable energy storage, Engineering, **21** (2023) 32–35. https://doi.org/10.1016/j.eng.2022.10.008

6. Zheng F, Kotobuki M, Song S, Lai MO, et al., Review on solid electrolytes for all-solid-state lithium-ion batteries, J. Power Sources, **389** (2018) 198–213. https://doi.org/10.1016/j.jpowsour.2018.04.022

7. Han Y, Chen Y, Huang Y, Zhang M, et al., Recent progress on garnet-type oxide electrolytes for all-solid-state lithium-ion batteries, Ceram. Int., **49(18)** (2023) 29375–29390. https://doi.org/10.1016/j.ceramint.2023.06.153

8. Yaroslavtsev AB, Solid electrolytes: main prospects of research and development, Russ. Chem. Rev., **85(11)** (2016), 1255. https://doi.org/10.1070/RCR4634

9. Murugan R, Thangadurai V, Weppner W, Fast lithium ion conduction in garnet-type $Li_7La_3Zr_2O_{12}$, Angew. Chem., **46(41)** (2007) 7778. https://doi.org/10.1002/anie.200701144

10. Ramakumar S, Deviannapoorani C, Dhivya L, Shankar LS, et al., Lithium garnets: Synthesis, structure, Li^+ conductivity, Li^+ dynamics and applications, Prog. Mater. Sci., **88** (2017) 325–411. https://doi.org/10.1016/j.pmatsci.2017.04.007

11. Il'ina E, Recent Strategies for Lithium-Ion Conductivity Improvement in $Li_7La_3Zr_2O_{12}$ Solid Electrolytes, Int. J. Mol. Sci., **24(16)** (2023) 12905. https://doi.org/10.3390/ijms241612905

12. Palakkathodi Kammampata S, Thangadurai V, Cruising in ceramics—discovering new structures for all-solid-state batteries—fundamentals, materials, and performances, Ionics, **24** (2018) 639–660. https://doi.org/10.1007/s11581-017-2372-7

13. Li W, Bao Z, Wang J, Du Q, et al., Comparative simulation of thin-film and bulk-type all-solid-state batteries under adiabatic and isothermal conditions, Appl. Therm. Eng., **223** (2023) 119957. https://doi.org/10.1016/j.applthermaleng.2022.119957

14. Xia Q, Zan F, Zhang Q, Liu W, et al., All-solid-state thin film lithium/lithium-ion microbatteries for powering the Internet of things, Adv. Mater., **35(2)** (2023) 2200538. https://doi.org/10.1002/adma.202200538

15. Wang C, Wang C, Li M, Zhang S, et al., Design of thin solid-state electrolyte films for safe and energy-dense batteries, Mater. Today, **72** (2023) 235–254. https://doi.org/10.1016/j.mattod.2023.11.016

16. Katsui H, Goto T, Impedance of cubic $Li_7La_3Zr_2O_{12}$ film deposited on strontium ruthenate substrate by chemical vapor deposition, Mater. Today: Proceedings, **4(11)** (2017) 11445–11448. https://doi.org/10.1016/j.matpr.2017.09.025

17. Loho C, Djenadic R, Mundt P, Clemens O, et al., On processing-structure-property relations and high ionic conductivity in garnet-type $Li_5La_3Ta_2O_{12}$ solid electrolyte thin films grown by CO_2-laser assisted CVD, Solid State Ion., **313** (2017) 32–44. https://doi.org/10.1016/j.ssi.2017.11.005

18. Loho C., Djenadic R, Bruns M, Clemens O, et al., Garnet-type $Li_7La_3Zr_2O_{12}$ solid electrolyte thin films grown by CO_2-laser assisted CVD for all-solid-state batteries, J. Electrochem. Soc., **164(1)** (2016) A6131. https://doi.org/10.1149/2.0201701jes

19. Katsui H, Goto T, Preparation of cubic and tetragonal $Li_7La_3Zr_2O_{12}$ film by metal organic chemical vapor deposition,

Thin Solid Films, **584** (2015) 130–134. https://doi.org/10.1016/j.tsf.2014.11.094

20. Kazyak E, Chen K-H, Wood KN, Davis AL, et al., Atomic layer deposition of the solid electrolyte garnet $Li_7La_3Zr_2O_{12}$, Chem. Mater., **29(8)** (2017) 3785–3792. https://doi.org/10.1021/acs.chemmater.7b00944

21. Lobe S, Dellen C, Finsterbusch M, Gehrke H-G, et al., Radio frequency magnetron sputtering of $Li_7La_3Zr_2O_{12}$ thin films for solid-state batteries, J. Power Sources, **307** (2016) 684–689. https://doi.org/10.1016/j.jpowsour.2015.12.054

22. Sastre J, Priebe A, Döbeli M, Michler J, et al., Lithium garnet $Li_7La_3Zr_2O_{12}$ electrolyte for all-solid-state batteries: closing the gap between bulk and thin film Li-ion conductivities, Adv. Mater. Interfaces, **7(17)** (2020) 2000425. https://doi.org/10.1002/admi.202000425

23. Sastre J, Futscher MH, Pompizi L, Aribia A, et al., Blocking lithium dendrite growth in solid-state batteries with an ultrathin amorphous Li-La-Zr-O solid electrolyte, Commun. Mater., **2(1)** (2021) 76. https://doi.org/10.1038/s43246-021-00177-4

24. Rawlence M, Garbayo I, Buecheler S, Rupp JLM, On the chemical stability of post-lithiated garnet Al-stabilized $Li_7La_3Zr_2O_{12}$ solid state electrolyte thin films, Nanoscale, **8(31)** (2016) 14746–14753. https://doi.org/10.1039/C6NR04162K

25. Tan J, Tiwari A, Characterization of $Li_7La_3Zr_2O_{12}$ thin films prepared by pulsed laser deposition, MRS Online Proceedings Library (OPL), **1471** (2012) mrss12-1471-yy03-04. https://doi.org/10.1557/opl.2012.1266

26. Koresh I, Tang Z, Troczynski T, A novel approach to prepare Li-La-Zr-O solid state electrolyte films by suspension plasma spray, Solid State Ion., **368** (2021) 115679. https://doi.org/10.1016/j.ssi.2021.115679

27. Tadanaga K, Egawa H, Hayashi A, Tatsumisago M, et al., Preparation of lithium ion conductive Al-doped $Li_7La_3Zr_2O_{12}$ thin films by a sol–gel process, J. Power Sources, **273** (2015) 844–847. https://doi.org/10.1016/j.jpowsour.2014.09.164

28. Bitzer M, Gestel TV, Uhlenbruck S, Buchkremer H-P, Sol-gel synthesis of thin solid $Li_7La_3Zr_2O_{12}$ electrolyte films for Li-ion batteries, Thin Solid Films, **615** (2016) 128–134. https://doi.org/10.1016/j.tsf.2016.07.010

29. Lyalin E, Il'ina E, Kalinina E, Antonov B, et al., Electrophoretic deposition and characterization of thin-film membranes $Li_7La_3Zr_2O_{12}$, Membranes, **13(5)** (2023) 468. https://doi.org/10.3390/membranes13050468

30. Lyalin E, Il'ina E, Pankratov A, Kuznetsova T, et al., Effect of Substrates on the Physicochemical Properties of $Li_7La_3Zr_2O_{12}$ Films Obtained by Electrophoretic Deposition, Micromachines, **14(12)** (2023) 2153. https://doi.org/10.3390/mi14122153

31. Mistler RE, Twiname ER. Tape casting: theory and practice. American ceramic society; 2000. 298 p.

32. Yi E, Wang W, Kieffer J, Laine RM, Flame made nanoparticles permit processing of dense, flexible, Li+ conducting ceramic electrolyte thin films of cubic-$Li_7La_3Zr_2O_{12}$ (c-LLZO), J. Mater. Chem. A, **4(33)** (2016) 12947–12954. https://doi.org/10.1039/C6TA04492A

33. Yi E, Wang W, Kieffer J, Laine RM, Key parameters governing the densification of cubic-$Li_7La_3Zr_2O_{12}$ Li^+ conductors, J. Power Sources, **352** (2017) 156–164. https://doi.org/10.1016/j.jpowsour.2017.03.126

34. Hanc E, Zając W, Lu L, Yan B, et al., On fabrication procedures of Li-ion conducting garnets, J. Solid State Chem., **248** (2017) 51–60. https://doi.org/10.1016/j.jssc.2017.01.017

35. Fu KK, Gong Y, Hitz GT, McOwen DW, et al., Three-dimensional bilayer garnet solid electrolyte based high energy density lithium metal–sulfur batteries, Energy Environ. Sci., **10(7)** (2017) 1568–1575. https://doi.org/10.1039/C7EE01004D

36. Liu B, Zhang L, Xu S, McOwen DW, et al., 3D lithium metal anodes hosted in asymmetric garnet frameworks toward high energy density batteries, Energy Storage Mater., **14** (2018) 376–382. https://doi.org/10.1016/j.ensm.2018.04.015

37. Jonson RA, McGinn PJ, Tape casting and sintering of $Li_7La_3Zr_{1.75}Nb_{0.25}Al_{0.1}O_{12}$ with Li_3BO_3 additions, Solid State Ion., **323** (2018) 49–55. https://doi.org/10.1016/j.ssi.2018.05.015

38. Gao K, He M, Li Y, Zhang Y, et al., Preparation of high-density garnet thin sheet electrolytes for all-solid-state Li-Metal batteries by tape-casting technique, J. Alloys Compd., **791** (2019) 923–928. https://doi.org/10.1016/j.jallcom.2019.03.409

39. Hitz GT, McOwen DW, Zhang L, Ma Z, et al., High-rate lithium cycling in a scalable trilayer Li-garnet-electrolyte architecture, Mater. Today, **22** (2019) 50–57. https://doi.org/10.1016/j.mattod.2018.04.004

40. Ye R, Tsai CL, Ihrig M, Sevinc S, et al., Water-based fabrication of garnet-based solid electrolyte separators for solid-state lithium batteries, Green Chem., **22(15)** (2020), 4952–4961. https://doi.org/10.1039/D0GC01009J

41. Fu Z, Zhang L, Gritton JE, Godbey G, et al., Probing the mechanical properties of a doped $Li_7La_3Zr_2O_{12}$ garnet thin electrolyte for solid-state batteries, ACS Appl. Mater. Interfaces, **12(22)** (2020) 24693–24700. https://doi.org/10.1021/acsami.0c01681

42. Hamao N, Hamamoto K Fabrication of single-grain-layered garnet-type electrolyte sheets by a precursor method, J. Asian Ceram. Soc., **10(1)** (2022) 1–8. https://doi.org/10.1080/21870764.2021.1974782

43. Parejiya A, Dixit MB, Parikh D, Amin R, et al., Understanding slurry formulations to guide solution-processing of solid electrolytes, J. Power Sources, **544** (2022) 231894. https://doi.org/10.1016/j.jpowsour.2022.231894

44. Bao C, Zheng C, Wu M, Zhang Y, et al., 12 μm-Thick Sintered Garnet Ceramic Skeleton Enabling High-Energy-Density Solid-State Lithium Metal Batteries, Adv. Energy Mater., **13(13)** (2023) 2204028. https://doi.org/10.1002/aenm.202204028

45. Xiang W, Ma R, Liu X, Kong X, et al., Rapid Li compensation toward highly conductive solid state electrolyte film, Nano Energy, **116** (2023) 108816. https://doi.org/10.1016/j.nanoen.2023.108816

46. Dai B, Zhou M, Liu K, He B, et al., The molding of the ceramic solid electrolyte sheet prepared by tape casting, J. Phys. Conf. Ser., **2566(1)** (2023) 012102. https://doi.org/10.1088/1742-6596/2566/1/012102

47. Jonson RA, Yi E, Shen F, Tucker MC, Optimization of tape casting for fabrication of $Li_{6.25}Al_{0.25}La_3Zr_2O_{12}$ sheets, Energy Fuels, **35(10)** (2021) 8982–8990. https://doi.org/10.1021/acs.energyfuels.1c00566